

First-principles modelling of molecular single-electron transistors

Kurt Stokbro*

QuantumWise A/S, Nørre Søgade 27A, 1. th, DK-1370 Copenhagen K, Denmark

E-mail: kurt.stokbro@quantumwise.com

Abstract

We present a first-principles method for calculating the charging energy of a molecular single-electron transistor operating in the Coulomb blockade regime. The properties of the molecule are modelled using density-functional theory, the environment is described by a continuum model, and the interaction between the molecule and the environment are included through the Poisson equation. The model is used to calculate the charge stability diagrams of a benzene and C₆₀ molecular single-electron transistor.

Introduction

The use of non-equilibrium Greens functions (NEGF) in connection with density-functional theory (DFT)¹⁻⁴ or semi-empirical models⁵⁻¹² has been highly successful in modelling coherent transport in various types of molecular junctions. However, in the case of molecular single-electron transistors (SET), the transport is incoherent,¹³ and another approach is needed. Kaasbjerg *et al.* introduced a semi-empirical model for simulating the properties of molecular SETs. In particular

*To whom correspondence should be addressed

they showed the importance of including renormalization of the molecular charge states due to the polarization of the environment.

In this paper we extend this framework to be included within a density-functional theory description of molecular SET's operating in the coulomb blockade regime. We use the model to calculate the charging energy of benzene and C_{60} in an electrostatic environment resembling a molecular SET geometry. We calculate the charging energy as function of an external gate potential, and from this we obtain the charge stability diagram of the two respective molecules.

The outline of the paper is as follows. In the first section we describe the basics of an SET, and in the following section the DFT framework for modelling the device. We next present calculations of the properties of benzene and C_{60} in an electrostatic environment, and in the final section we summarize the results.

Basic theory of a molecular single electron transistor

[figure][1][1]a schematically illustrates the geometry of a nanoscale molecular transistor. The geometry consists of metallic source and drain electrodes, and a molecular island coupled with the two electrodes. Electrons can propagate from source to drain through the island.

If the island is strongly coupled with the source and drain electrodes, the electrons will stay a very short time on the island, and cannot localize but will move coherently through the system. This is the regime where we can use the coherent transport model for simulating the electrical properties of the system. This is the situation shown in [figure][1][1]b, and we note that a current can flow through the system even when the island does not have any electronic states within the bias window, as illustrated in the figure by the finite lifetime-broadened lowest unoccupied molecular orbital (LUMO), which the carrier can use for propagating from left to right.

In this paper, we will investigate the regime where the island is weakly coupled with the electrodes. In this case, the electron tunnels from the source to the island and stays there for sufficiently long time to localize. The electron thereby loses all information about its original quantum state.

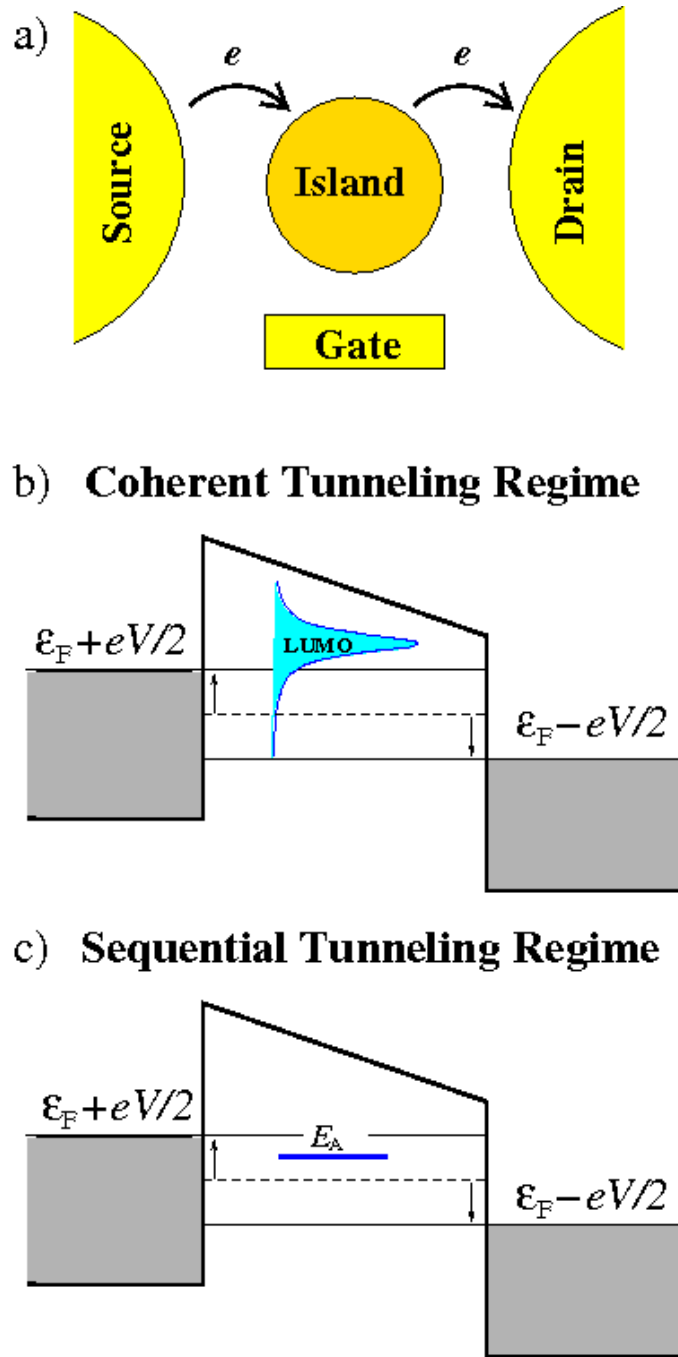


Figure 1: (Color online) a) Schematics of a nanoscale transistor. Electrons propagate from the source to the drain through an island. The energies of the electronic states on the island can be controlled by an electrostatic gate. b) In the strong coupling regime, the electron propagates coherently through the device, and the electronic states of the island have a finite lifetime and therefore a finite width. c) In the weak coupling regime, the electron localizes on the island and propagates by sequential tunneling. The electronic states on the island are in this case discrete.

Thus, the subsequent tunneling process from the island to the drain electrode will be independent from the tunneling process into the island. This transport mechanism is referred to as sequential tunneling and is depicted in [figure][1][1]c. Electron transport is in this case only possible if the island has an electronic level within the bias window, as illustrated by the electron affinity level (EA) in [figure][1][1]. As in the coherent case, the position of the molecular levels and in particular the electron affinity level can be adjusted by an external gate potential, and by appropriate tuning, the island can in this regime thus be opened or closed for transport. For source-drain voltages below the charging energy of the island, there will only be one energy level within the bias window, and the system will work as a single electron transistor, as desired for our present discussion.

The energy balance in the weak coupling regime

In the following we will focus on the weak coupling regime where the transport is described by sequential tunneling. We introduce the function $E^{\text{island}}(N)$, which gives the total energy of the island as function of the number of electrons on the island. We also introduce similar energy functions for the source and drain electrodes, $E^{\text{source}}(N)$ and $E^{\text{drain}}(N)$.

For the electron to move from the source electrode onto the island, the electron must have a lower energy on the island, i.e.

$$E^{\text{source}}(M) + E^{\text{island}}(N) \geq E^{\text{source}}(M - 1) + E^{\text{island}}(N + 1), \quad (1)$$

where N and M are the initial number of electrons on the island and in the source electrode, respectively.

Moreover, in order to move the electron from the island to the drain electrode, it must have a lower energy in the drain electrode,

$$E^{\text{drain}}(K) + E^{\text{island}}(N + 1) \geq E^{\text{drain}}(K + 1) + E^{\text{island}}(N), \quad (2)$$

where K is the initial number of electrons in the drain electrode.

The maximum energy of the electron in the source electrode is $-W + eV/2$, where W is the work function of the electrode and V the applied bias. Assuming that the electron with maximum energy tunnels onto the island, then we have

$$E^{\text{source}}(M) - E^{\text{source}}(M-1) = -W + eV/2. \quad (3)$$

Using the above tunneling criterion, we obtain the condition

$$-W + eV/2 + E^{\text{island}}(N) \geq E^{\text{island}}(N+1). \quad (4)$$

Similarly, $-W - eV/2$ is the minimum energy of an electron in the drain electrode, and thus

$$E^{\text{island}}(N+1) \geq -W - eV/2 + E^{\text{island}}(N). \quad (5)$$

The requirement for a current to flow in the device is therefore

$$e|V|/2 \geq \Delta E^{\text{island}}(N) + W \geq -e|V|/2, \quad (6)$$

where $\Delta E^{\text{island}}(N) = E^{\text{island}}(N+1) - E^{\text{island}}(N)$ is the charging energy of the island.

In the following we will calculate the charging energy of two different molecular SETs and use [equation][6][6] to obtain the so-called charge stability diagram, which shows the number of charge states inside the bias window as function of the gate and source-drain voltages.

Total energy of a molecule in an electrostatic environment

In this section we will discuss the calculation of the total energy of a molecule in an electrostatic environment. All calculations are performed using the commercial software package Atomistix ToolKit (ATK).¹⁴ The DFT model in ATK is based on pseudopotentials with numerical localized basis functions using the method outlined by Soler *et al.*¹⁵ In this framework, a compensation

charge $\rho_i^{\text{comp}}(\mathbf{r})$ is introduced for each atomic site. The compensation charge has the same charge Z_i as the pseudopotential, and is used to screen the electrostatic interactions.

We now introduce the electron difference density

$$\delta n(\mathbf{r}) = n(\mathbf{r}) - \sum_i \rho_i^{\text{comp}}(\mathbf{r}), \quad (7)$$

where $n(\mathbf{r})$ is the total charge density of the system. We also introduce the screened (“neutral atom”) local pseudopotential

$$V_i^{\text{NA}}(\mathbf{r}) = V_i^{\text{loc}}(\mathbf{r}) - \int \frac{\rho_i^{\text{comp}}(\mathbf{r}')}{|\mathbf{r} - \mathbf{r}'|} d\mathbf{r}', \quad (8)$$

where V_i^{loc} is the local pseudopotential at site i .

Following Ref. 15, we rearrange the terms to obtain the DFT total-energy functional

$$E[n] = T[n] + E^{\text{xc}}[n] + \frac{1}{2} \int \delta V^{\text{H}}(\mathbf{r}) \delta n(\mathbf{r}) d\mathbf{r} + \int \sum_i V_i^{\text{NA}}(\mathbf{r}) \delta n(\mathbf{r}) d\mathbf{r} + \frac{1}{2} \sum_{ij} U_{ij}, \quad (9)$$

where T is the one-electron kinetic energy, E^{xc} the exchange-correlation energy, and the three last terms are the rearranged electrostatic terms. The first of these is the relative Hartree energy, and is obtained from the difference Hartree potential $\delta V^{\text{H}}(\mathbf{r})$ which is calculated by solving the Poisson equation for the difference density $\delta n(\mathbf{r})$. The next term describes the relative external energy, while the last term contains all the electrostatic interactions which do not depend on the electron density. The last term is calculated from V_i^{loc} , ρ_i^{comp} , and Z_i , and since the Poisson equation is linear, this term can be decomposed into the pair-potential U_{ij} .

We next extend the total-energy functional to include interactions with a number of dielectric and metallic regions surrounding the molecular system. [figure][2][2 illustrates a typical molecular single electron transistor geometry where a benzene molecule is positioned on top of a dielectric material and surrounded by three metallic electrodes. Within the metallic regions the potential is fixed to the applied voltage on each respective electrode.

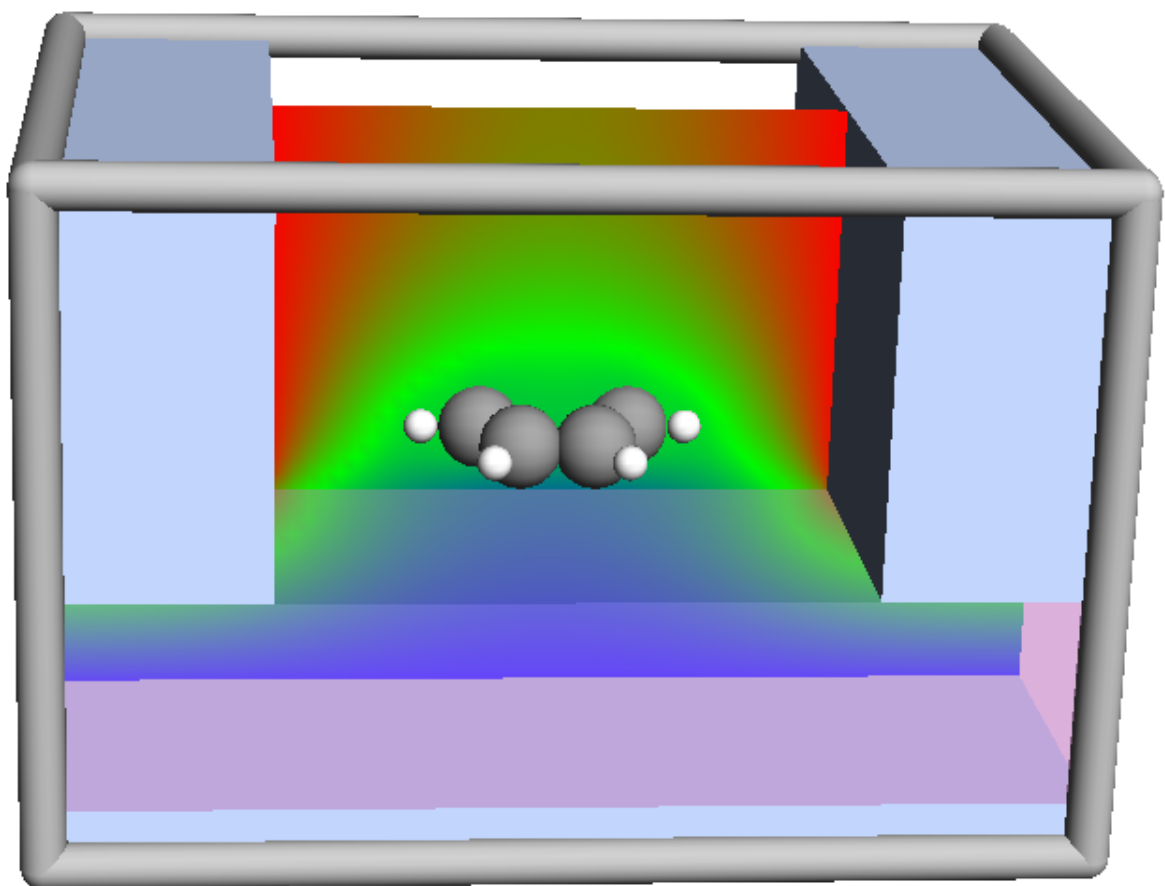


Figure 2: (Color online) A benzene molecule in the SET environment considered in this paper. The electrostatic environment models two metallic electrodes (source and drain) on top of a dielectric substrate with a metallic back-gate. The contour plot shows the induced electrostatic potential for a gate voltage of 2 V and zero source-drain bias.

Solving the Poisson equation without the molecule present, we obtain the external potential from the electrostatic environment,

$$-\nabla \cdot [\boldsymbol{\varepsilon}(\mathbf{r}) \nabla V^{\text{ext}}(\mathbf{r})] = 0. \quad (10)$$

Adding the molecule to the geometry, we again solve the Poisson equation, but now with the electron difference density on the molecule, to obtain the total difference Hartree potential

$$-\nabla \cdot [\boldsymbol{\varepsilon}(\mathbf{r}) \nabla \delta V^{\text{H+ext}}(\mathbf{r})] = \delta n(\mathbf{r}). \quad (11)$$

Finally, we define the molecular part of the total difference Hartree potential

$$\delta V^{\text{H}}(\mathbf{r}) = \delta V^{\text{H+ext}}(\mathbf{r}) - V^{\text{ext}}(\mathbf{r}), \quad (12)$$

and this is the difference Hartree potential which enters into [equation][9][9]. Following Neugebauer and Scheffler,¹⁶ we add the energy contribution from the external field through the term

$$\Delta E = \int V^{\text{ext}}(\mathbf{r}) n(\mathbf{r}) d(\mathbf{r}) - \sum_i V^{\text{ext}}(\mathbf{R}_i) Z_i, \quad (13)$$

where \mathbf{R}_i is the position of site i , and Z_i the valency of the pseudopotential at site i .

Thus, the total energy is given by adding the contributions from [equation][9][9] and [equation][13][13]. Note that this is only exact if the last electro-static pair-potential term in [equation][9][9] is unaffected by the electrostatic surroundings, which is the case if the compensation charge and the screened local pseudopotential do not overlap with the metallic and dielectric regions.

Results

We will now present results for the charging energy of a benzene and C_{60} molecule in an SET geometry. To obtain some reference energies, we will first calculate the charging energies of the isolated molecules. We obtain the charging energy by performing self-consistent calculations for the N and $N + 1$ charge states of the isolated molecule and subtracting their total energies. For the calculation we use non-polarized DFT in the local density approximation (LDA)¹⁷ and expand the wavefunctions in a double-zeta polarized (DZP) basis set. The molecular geometries were obtained by relaxing the molecules in the neutral state.

Table 1: Experimental ionization (I) and affinity (A) energies for benzene and C_{60} molecules compared with theoretical DFT-LDA values. The theoretical values denoted “isolated” are obtained from the total energies of the charged isolated molecule. The “SET” values are obtained by calculating the total energy of the charged molecule in the electrostatic surrounding illustrated in [figure][2][2], at zero gate and source-drain bias.

benzene	E_I^{+1}	E_I	E_A	E_A^{-1}
Exp.		9.25 ¹⁸		
isolated	15.73	9.15	-2.34	-8.39
SET	7.70	5.41	-2.26	-4.88
C_{60}	E_I^{+1}	E_I	E_A	E_A^{-1}
Exp.	11.33 ¹⁹	7.65 ¹⁹	2.65 ²⁰	
isolated	10.09	6.84	1.90	-1.32
SET	7.24	5.89	2.85	1.53

[table][1][1] shows the calculated charging energies. For benzene there is excellent agreement with the experimental results, while the results for C_{60} are about 1 eV too small. To investigate possible origins of this discrepancy we performed calculations where C_{60} was allowed to spin polarize and relaxed the molecule also in the charged state. We found that such effects change the total energy by less than 0.1 eV, and can therefore safely be disregarded.

We next set up the molecules in the SET electrostatic environment. The geometry is illustrated in [figure][2][2]. It consists of a metallic back-gate, and above the gate there is 3.8 Å of dielectric material with dielectric constant $10\epsilon_0$. The molecule is positioned 1.2 Å above the dielectric. To the left and right of the molecule are metallic source-drain electrodes, and the distance between

the molecule and the electrodes is 2.8 Å. We note that for a typical metal surface the image plane is 2 Å above the surface,²¹ and to compare with atomic adsorption geometries this length must be added to the above distances.

[table][1][1] lists the charging energies of the molecules in the SET environment with zero potential at the gate electrode. We see that for benzene the charging energy is strongly reduced, while the effect is smaller for C₆₀. The reduction in charging energy arises from the screening of the charged molecule by the surrounding dielectric and metal electrodes.²²

For benzene we may compare with the GW calculations by Neaton *et al.*²³ They find the gas phase value for $E_{\text{LUMO}} - E_{\text{HOMO}} = 10.51$ eV and for benzene adsorbed on graphene $E_{\text{LUMO}} - E_{\text{HOMO}} = 7.35$ eV, which is comparable with our values of $E_{\text{I}} - E_{\text{A}} = 11.49$ eV in the gas phase and $E_{\text{I}} - E_{\text{A}} = 7.67$ eV in the SET environment.

We next calculate the total energy of the different charge states of the SET system as function of the gate potential. The results are shown in [figure][3][3]. The total energy includes the reservoir energy qW , where q is the charge of the molecule and W is the work function of the electrode; we use the value $W = 5.28$ eV which models a gold electrode.²⁴

[figure][3][3] shows that the neutral molecule has the lowest energy at zero gate potential. At negative gate potentials the positive charge states are stabilized, while the negative charge states are stabilized at positive gate potentials. This is in agreement with that HOMO and LUMO levels follow $-eV_G$, thus, at positive bias the LUMO level gets below the electrode Fermi level and attracts an electron, and the molecule becomes negatively charged. At negative gate potentials the HOMO level gets above the electrode Fermi level and an electron is escaping from the molecule, which becomes positively charged.

To understand the dependence between the total energy and the gate potential we fit a quadratic function to the data

$$E = \alpha q V_G + \beta (e V_G)^2. \quad (14)$$

Note that we assume the linear term to be proportional to the charge q on the molecule, while the quadratic term arises from polarization of the molecule and therefore is independent of q . By

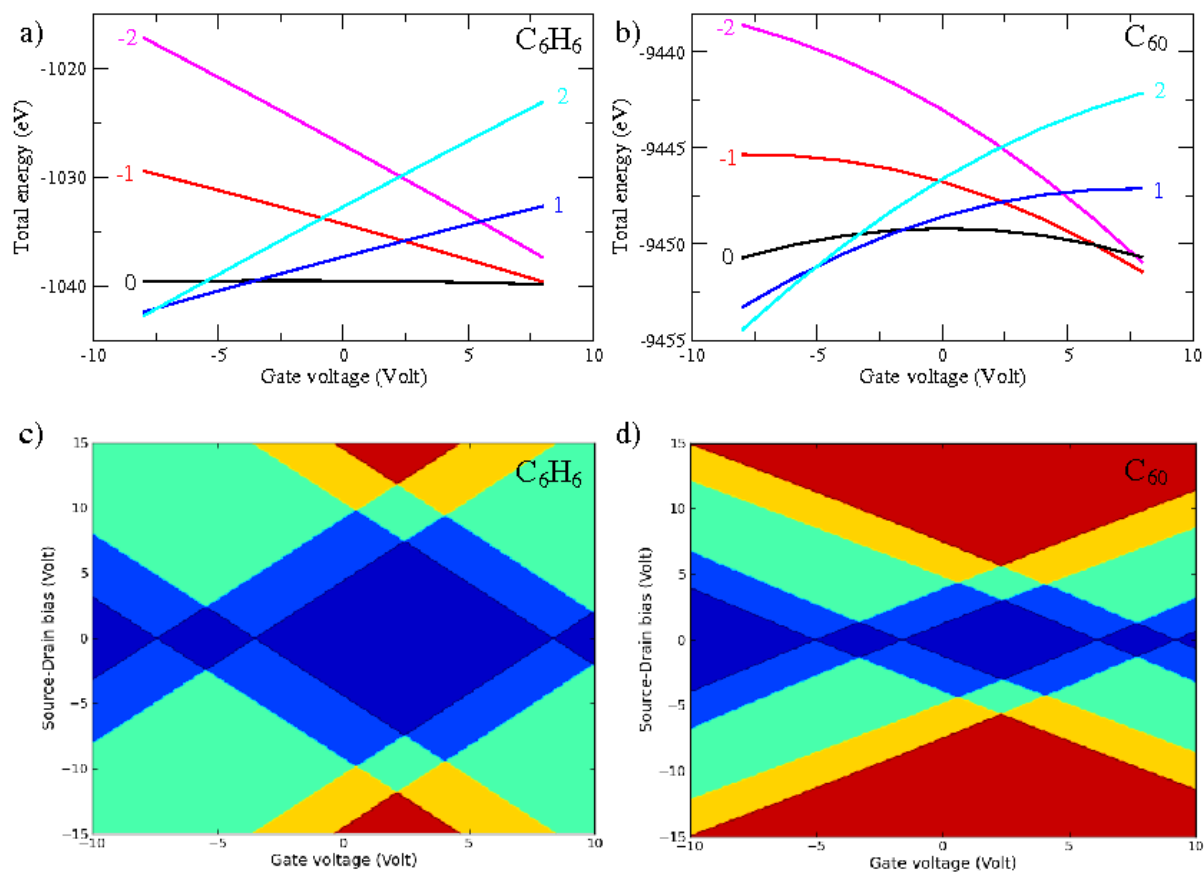


Figure 3: (Color online) a) Total energy as function of the gate voltage for the benzene molecule, in the SET environment. Different curves are for charge states -2 , -1 , 0 , 1 , 2 . c) Charge stability diagram; the color shows the number of charge states within the bias window for a given gate voltage and source-drain bias. dark blue(0), blue(1), green(2), yellow(3), red(4). b) and d) shows similar plots for the C_{60} molecule, in the SET environment.

fitting the data in [figure][3][3] we find for benzene $\alpha = 0.62$ eV, $\beta = -0.003$ eV⁻¹, and for C₆₀ $\alpha = 0.38$ eV, $\beta = -0.025$ eV⁻¹, where the variation with the charge state is ~ 0.01 eV for α and ~ 0.001 eV⁻¹ for β .

Thus, benzene is stronger coupled with the gate than C₆₀, because the benzene atoms on average are closer to the dielectric substrate. Therefore, the benzene molecule shows an almost linear relationship between the total energy and the gate potential, since all atoms are almost identically shifted by the gate potential.

For C₆₀, on the other hand, the relationship between the total energy and the gate potential is non-linear. For this molecule the atoms closest to the dielectric region screen the gate potential for the rest of the molecule, and thus the gate coupling becomes smaller. A difference in the charges on different atoms in the molecule gives rise to a molecular dipole, and it is this polarization energy that gives the second-order contribution to the total energy.

From the total energies we can finally calculate the charge stability diagram using [equation][6][6]. The result is shown in [figure][3][3]c,d. The different colors show the number of charge states in the bias window. We see that the excitation energy for C₆₀ is smaller than for benzene. For both systems the excitation energy of the second electron is much smaller than for the first electron. We also note that the non-linear dependence of the total energy on the gate potential for C₆₀ is not observable in the charge stability diagram. This is because the charge stability diagram only depends on the energy differences between the charge states, and the second-order term in [equation][14][14] is independent on the charge state.

Conclusions

We have in this paper demonstrated the use of density-functional theory for calculating the charging energy of a molecule in a metallic environment that models the geometry of a molecular single-electron transistor. We find that the metallic environment reduces the charging energy of the molecules, in agreement with GW²³ and Hückel²² calculations. We calculated the charging

energy as function of the gate potential and from this obtained the charge stability diagram. The simulations show how DFT can be used to gain new insight into the properties of molecular single-electron transistors operating in the coulomb blockade regime.

Acknowledgement

This work was supported by the Danish Council for Strategic Research 'NABIIT' under Grant No. 2106-04-0017, "Parallel Algorithms for Computational Nano-Science", and European Commission STREP project No. MODECOM "NMP-CT-2006-016434", EU. I would also like to thank Anders Blom for important comments to the manuscript.

References

- (1) Lang, N. D. *Phys. Rev. B* **1995**, *52*, 5335.
- (2) Xue, Y. *Chemical Physics* **2002**, *281*, 151–170.
- (3) Brandbyge, M.; Mozos, J.-L.; Ordejón, P.; Taylor, J.; Stokbro, K. *Phys. Rev. B* **2002**, *65*, 165401.
- (4) Taylor, J.; Guo, H.; Wang, J. *Phys. Rev. B* **2001**, *63*, 245407.
- (5) Magoga, M.; Joachim, C. *Phys. Rev. B* **1997**, *56*, 4722.
- (6) Corbel, S.; Cerdá, J.; Sautet, P. *Phys. Rev. B* **1999**, *60*, 1989.
- (7) Cerdá, J.; Soria, F. *Phys. Rev. B* **2000**, *61*, 7965–7971.
- (8) Emberly, E. G.; Kirczenow, G. *Phys. Rev. B* **2001**, *62*, 10451.
- (9) Zahid, F.; Paulsson, M.; Polizzi, E.; Ghosh, A. W.; Siddiqui, L.; Datta, S. *J. of Chem. Phys.* **2005**, *123*, 064707.
- (10) Kienle, D.; Cerdá, J. I.; Ghosh, A. W. *J. Appl. Phys.* **2006**, *100*, 043714.

- (11) Kienle, D.; Bevan, K. H.; Liang, G.-C.; Siddiqui, L.; Cerdá, J. I.; Ghosh, A. W. *J. Appl. Phys.* **2006**, *100*, 043715.
- (12) Stokbro, K.; Petersen, D. E.; Smidstrup, S.; Blom, A.; Ipsen, M.; Kaasbjerg, K. Submitted, arXiv:1004.2812v1 (<http://arxiv.org/abs/1004.2812>).
- (13) Kubatkin, S.; Danilov, A.; Hjort, M.; Cornil, J.; Bredas, J.-L.; Stuhr-Hansen, N.; Hedegård, P.; Bjørnholm, T. *Nature* **2003**, *425*, 698.
- (14) Atomistix ToolKit version 2010.02, QuantumWise A/S (<http://quantumwise.com/>).
- (15) Soler, J. M.; Artacho, E.; Gale, J. D.; García, A.; Junquera, J.; Ordejón, P.; Sánchez-Portal, D. *Journal of Physics: Condensed Matter* **2002**, *14*, 2745–2779.
- (16) Neugebauer, J.; Scheffler, M. *Phys. Rev. B* **1992**, *46*, 16067.
- (17) Perdew, J. P.; Zunger, A. *Phys. Rev. B* **1981**, *23*, 5048–5079.
- (18) Lias, S. G.; Bartmess, J. E.; Liebman, J. E.; Holmes, J. L.; Levin, R. D.; Mallard, W. G. *J. Phys. Chem. Ref. Data* **1988**, *17* (suppl 1), year.
- (19) Pogulay, A. V.; Abzalimov, R. R.; Nasibullaev, S. K.; Lobach, A. S.; Drewello, T.; Vasilév, Y. V. *Int. J. of Mass Spec.* **2004**, *233*, 165.
- (20) Tosatti, E.; Manini, N. *Chem. Phys. Lett.* **1994**, *223*, 61.
- (21) Chulkov, E.; Silkin, V.; Echenique, P. *Surface Science* **1999**, *437*, 330.
- (22) Kaasbjerg, K.; Flensberg, K. *Nano Lett.* **2008**, *8*, 3809.
- (23) Neaton, J. B.; Hybertsen, M. S.; Louie, S. G. *Phys. Rev. Lett.* **2006**, *97*, 216405.
- (24) Rivière, J. C. *Appl. Phys. Lett.* **1966**, *8*, 172.